FINITE ELEMENT MODELLING OF INDUCTIVE SENSORS

J.K. Sykulski and R.L. Stoll

Department of Electrical Engineering
University of Southampton, UK

Abstract

Practical aspects of finite–element modelling of magnetic fields and calculating integral parameters such as a reflected impedance in inductive sensing devices are discussed. The electromagnetics of such sensors is briefly explained and some practical modelling techniques are put forward. Excellent agreement with experiment is reported.

1. Introduction

The operation of inductive sensors and detectors is based on a simple principle of detecting changes in the reflected impedance of the coil due to disturbances in magnetic field caused by the proximity of conducting/magnetic materials. A typical undisturbed field pattern for the sort of configuration under study is given in Fig. 1.
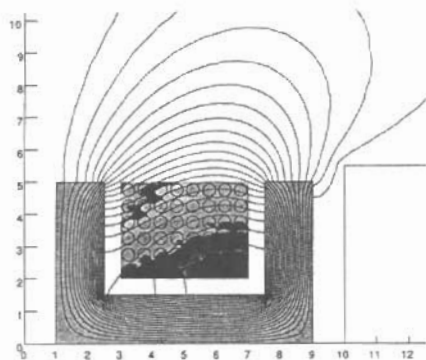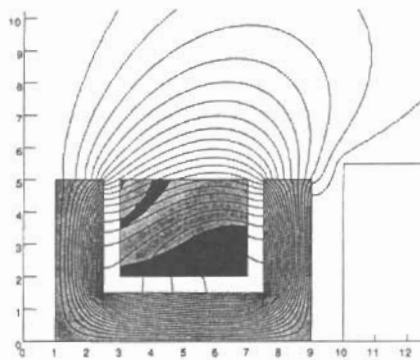

Fig. 1. *Field due to 48 turns*

Fig. 2. *Field due to 1 'big' turn*

The proximity of a magnetic/conducting object will influence the field distribution. The total reluctance of the system will be affected: both the value and the distribution of the flux will be changed. There are two basic mechanisms which will contribute to these changes. *The magnetic effect* If the target is made from magnetic but non–conducting material of high permeability, the total reluctance of the system will be reduced thus increasing the total flux generated by the same ampere–turns. The inductance of the coil will be increased. *The electric effect* In a non–magnetic but conducting target eddy–currents will be induced preventing the flux from entering the space previously available. A conducting target will therefore 'repel' the flux and force it to go through a region of a smaller cross–sectional area. This will cause a reduction in the value of the total flux and thus a reduction of inductance.

Some targets will fall into one of the above categories: copper or aluminium materials, for example, will exhibit only eddy–current effect. For such targets additional simplifying assumptions may be available with little or no loss in accuracy of computation. An iron target, on the other hand, is more difficult to modell as it produces both effects at the same time. Unsaturated iron is likely to produce a dominating magnetic effect hindered by the opposing influence of eddy–currents. As the eddy–current effect becomes stronger (due to increase in frequency or material conductivity) the magnetic flux attracted by the high permeability of iron will be confined to a very thin 'skin' on the surface, thus increasing considerably the flux density in that skin. A measure of this skin effect is given by the well–known eddy–current skin depth parameter $\delta=(\pi f \sigma \mu_0 \mu_r)^{-\frac{1}{2}}$. The high flux density in the skin will lead to local magnetic saturation which is likely to reduce substantially the 'effective' permeabilty of the iron, although the increased value of δ will act against this effect somewhat. Having established the level of saturation a simplified linear steady–state model may then be used with little loss of accuracy.

From the above physical insight it emerges that a variation of inductance with target distance is to be expected, subject to different material properties of the target combined with frequency of excitation. Magnetic but non–conducting materials should give an increase of coil inductance as the target is brought closer to the coil. Purely conducting (non–magnetic) targets will cause the inductance to fall. Iron targets may produce a variety of responses depending on the frequency. For higher frequencies, due to the 'skin effect' and local saturation, the two opposing effects (magnetic and electric) may even cancel out giving virtually no change of inductance with target range.

The *'effective'* resistance of the coil consists of two parts: the resistance of the coil itself at given frequency (with a possibility of a *'skin effect'* in the conductor, *'proximity effect'* in the coil and *'eddy current effect'* in other conducting parts of the system) plus a term representing power loss in the conducting target, which is always positive.

In the following calculations a typical sensor geometry has been assumed and dimensions chosen to emphasize various effects. Similar calculations conducted for a particular commercial sensor have shown excellent agreement with experimental data, thus validating the techniques and simplifications adopted.

2. Finite element modelling

Existing finite–element codes allow, in principle, a full transient time–stepping solution to accomodate the non–linear magnetic and eddy–current effects and to take account of detailed geometry. This leads, however, to long and cumbersome calculations, which may not be acceptable for design and development purposes. Simplifications and special modelling techniques are sought to make the process faster and truly interactive. It is usually sufficient, for example, to work in the frequency rather than the time domain and to use linearised magnetic characteristics with saturation either ignored or represented using an 'effective' permeability which may be estimated independently.

Further savings can be made by ignoring the presence of individual conductors in the coil and modelling it with one big conductor carrying current equal to the ampere–turns of the original coil. There is a dramatic reduction of number of elements required for modelling. As far as the magnetic field is concerned, the two models give almost identical field distribution (Figs 1 and 2). However, this simplifictaion has some impact on the coil proximity loss calculations (see Section 3).

The presence of a non–magnetic conducting target at high frequency and hence small skin depth can be represented in a simplified way by a 'cavity' with the Dirichlet boundary condition $A=0$, where A is the component of magnetic vector potential perpendicular to the plane of the mesh, ie parallel to the current. Such a condition prevents the magnetic flux from entering the 'cavity' in the way the real copper or brass material at high frequency prevents the entry of flux. The effect is equivalent to that of a superconductor where the flux is excluded at any frequency including zero. A much simpler mesh is then required (Fig. 4) as there is no longer a need for accurate modelling of the skin depth. For comparison of field plots see Figures 5 and 6.
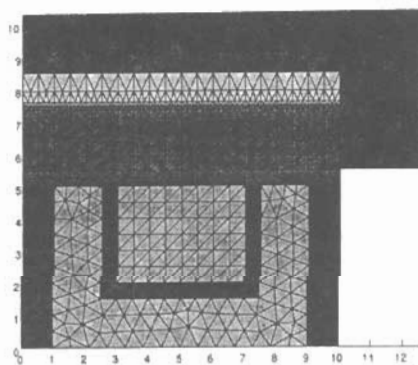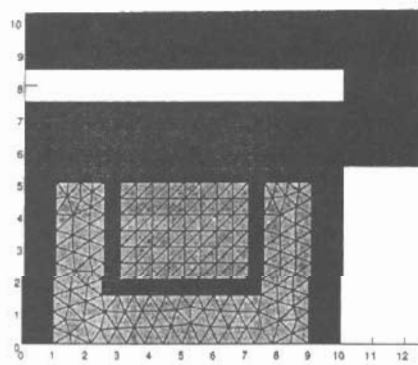

Fig. 3. *FE mesh with meshed target*   Fig. 4. *A 'cavity' model*

The resulting FE model is well suited for interactive CAD purposes. It is simple, fast, and, as comparison with measurements for a particular sensor has shown, very accurate. Examples of field distributions for different targets are shown in Figures 5 to 8.
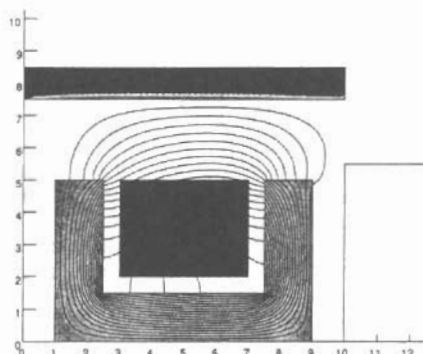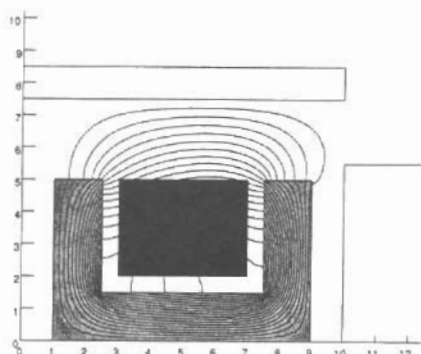

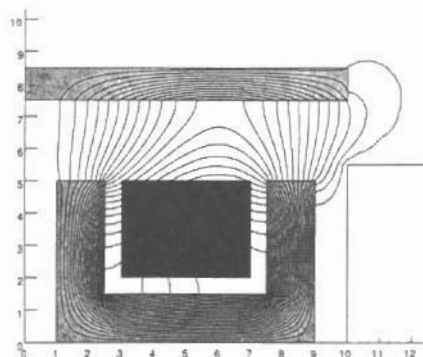Fig. 5. *Conducting target*

Fig. 6. *A 'cavity' model*

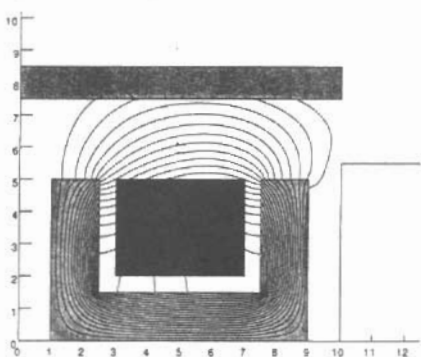
Fig. 7. *Magnetic target*

Fig. 8. *Iron target*

3. Calculation of reflected impedance

The inductance of the coil can be easily found from the FE solution through integration of the stored (or supplied) energy W. An appropriate post-processing command is usually available. The stored energy is then expressed in terms of inductance $W = \frac{1}{2}Li^2$.

The 'effective' resistance of the coil may be expressed as

$$R = R_{dc} + R_{skin} + R_{prox} + R_{other} + R_{target}$$

where R_{dc} is the *dc* resistance of the wire, R_{skin} represents the *skin effect* power loss in the conductor, R_{prox} is due to proximity effect in the coil conductors, R_{other} includes power loss in all other conducting parts of the sensor (mounting tube, etc), and R_{target} is the variable component due to power loss in the target. All the separate power losses can be calculated directly at the post-processing stage using appropriate volume (or area in the 2D case) integration commands – but only if a full FE model is used with all regions meshed and individual conductors in the coil are represented.

If the coil is modelled as one 'big' turn, the *skin effect* in the actual wire can be accounted for with good accuracy by using the well-known approximation for the resistance-limited case of a wire of radius a carrying a.c. current:

$$\frac{R_{ac}}{R_{dc}} = 1 + \frac{1}{48} \left\{ \frac{a}{\delta} \right\}^4$$

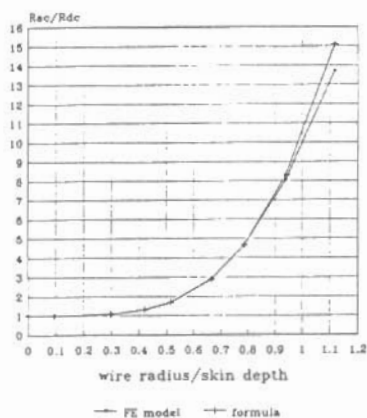because the frequency will always be such that $\delta > a$.

Fig. 9. *Proximity loss resistance*

The *proximity effect* calculation can be based on a solution for a conductor with circular cross-section in a uniform transverse field B: $w = 0.25\pi a^4 B^2 \omega^2 \sigma$ watts per metre, where σ is the conductivity of wire. After some modifications the following formula has been used:

$$R_{prox} = 0.9 \times \frac{\pi^2}{2} \frac{N}{S} \omega^2 a^4 \sigma \int_S rB^2 \ ds$$

which again involves using a post-processing integration command. N is the number of turns and S the cross-sectional area of the coil. The factor 0.9 is due to a non-uniform field distribution inside the conductor. The above formula gives remarkably good answers as shown in Fig. 9.

The inductance calculated using the 'cavity' model will be the same for different target materials, since the cavity does not recognise the type of material, only the fact that it is a good conductor. Calculation of resistance in this case involves integrating the square of the tangential component of magnetic field intensity over the surface of the cavity. The following equation can be used:

$$R_{target} = \frac{\pi}{i^2 \sigma \delta} \int rH_t^2 \ dl$$

and surfaces where the field is very weak may be ignored. A similar equation may be used when calculating R_{other} if a cavity model is used for these parts.
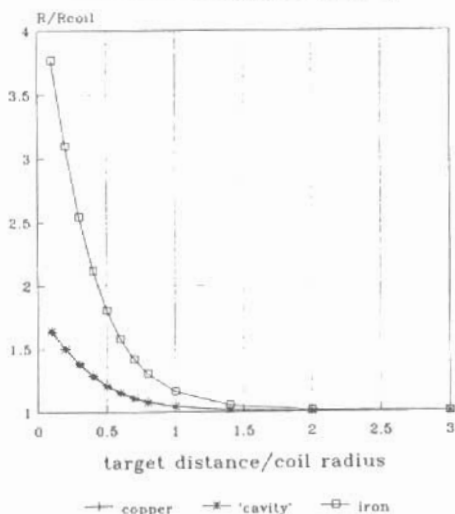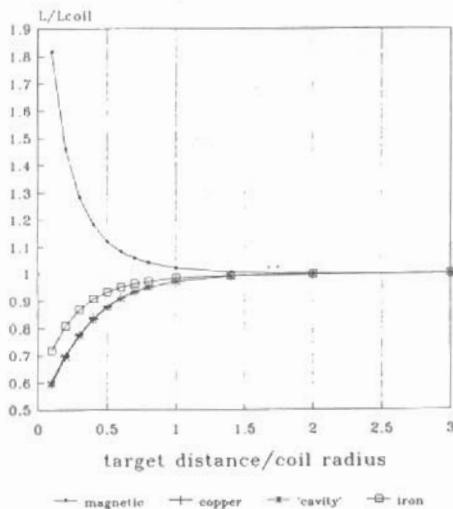

Fig 10. *Change of resistance*

Fig. 11. *Change of inductance*

Typical variations of coil inductance and resistance with changing position of the target are shown in Figures 10 and 11. L_{coil} and R_{coil} are the inductance and resistance of the coil when no target is present, and both Figures show relative changes of L and R due to bringing in the target. As mentioned earlier, similar calculations performed for a commercial sensor have shown very good agreement with experimental values.

Acknowledgement